Carbohydrate Polymers 190 (2018) 139–147

Contents lists available at ScienceDirect

Carbohydrate Polymers

journal homepage: www.elsevier.com/locate/carbpol

Spin-coating: A new approach for improving dispersion of cellulose nanocrystals and mechanical properties of poly (lactic acid) composites

Jamileh Shojaeiarani[a,*], Dilpreet S. Bajwa[a], Nicole M. Stark[b]

[a] Department of Mechanical Engineering, North Dakota State University, Fargo, ND 58102, United States
[b] U.S. Forest Service, Forest Products Laboratory, Madison, WI 53726-2398, United States

ARTICLE INFO

Keywords:
Poly(lactic acid)
Cellulose nanocrystals
Masterbatch
Composites
Solvent casting
Spin-coating

ABSTRACT

This study systematically evaluated the influence of masterbatch preparation techniques, solvent casting and spin-coating methods, on composite properties. Composites were manufactured by combining CNCs masterbatches and PLA resin using twin screw extruder followed by injection molding. Different microscopy techniques were used to investigate the dispersion of CNCs in masterbatches and composites. Thermal, thermomechanical, and mechanical properties of composites were evaluated. Scanning electron microscopy (SEM) images showed superior dispersion of CNCs in spin-coated masterbatches compared to solvent cast masterbatches. At lower CNCs concentrations, both SEM and optical microscope images confirmed more uniform CNCs dispersion in spin-coated composites than solvent cast samples. Degree of crystallinity of PLA exhibited a major enhancement by 147% and 380% in solvent cast and spin-coated composites, respectively. Spin-coated composites with lower CNCs concentration exhibited a noticeable improvement in mechanical properties. However, lower thermal characteristics in spin-coated composites were observed, which could be attributed to the residual solvents in masterbatches.

1. Introduction

During the past decade, the use of biocompatible and biodegradable materials has grown, primarily motivated by environmental consciousness and use of renewable resources (Cheng, Deng, Chen, & Ruan, 2009). Among the bio-based polymers, polylactic acid (PLA), which is derived from renewable resource, is widely used for commercial products (Drumright, Gruber, & Henton, 2000; Jamshidian, Tehrany, Imran, Jacquot, & Desobry, 2010; Lim, Auras, & Rubino, 2008; Masutani & Kimura, 2014; Nam, Sinha Ray, & Okamoto, 2003). Its biocompatible nature, relatively high strength, great wrinkle resistance and low toxicity are some beneficial characteristics that make PLA a promising alternative to petrochemical plastics (Domenek & Ducruet, 2016; Gupta, Simmons, Schueneman, Hylton, & Mintz, 2017; Oksman, Skrifvars, & Selin, 2003). However, its shortcomings such as low impact strength, high brittleness, low tensile elongation, and low heat degradation temperature limit the application of PLA (Li et al., 2014; Ljungberg & Wesslén, 2005; Shi, Jiang, Sun, & Gan, 2011; Yoon & Ji, 2003). Therefore, numerous methods have been tried to overcome these aforementioned weaknesses by using multiple reinforcing agents (De France, Chan, Cranston, & Hoare, 2016; Martínez-Sanz, Lopez-Rubio, & Lagaron, 2012; Shi et al., 2012; Yu et al., 2012).

Cellulose nanocrystals (CNCs) have attracted great interest due to their biocompatibility, low density, abundance, large surface area, and high strength in the composites field (Brinchi, Cotana, Fortunati, & Kenny, 2013; Lin, Huang, Chang, Feng, & Yu, 2011; Sullivan, Moon, & Kalaitzidou, 2015). Incorporation of CNCs in a polymeric matrix is expected to improve the mechanical and barrier properties of the matrix (Duran, Paula Lemes, & Seabra, 2012; Hamad, 2006; Klemm et al., 2011).

One of the main problems related to the use of CNCs as reinforcing agents is their high hydrophilicity and strong tendency to form aggregates in hydrophobic media (López de Dicastillo et al., 2017). Therefore, several techniques have been experimented to improve the dispersion of CNCs in polymer matrices. The most extended approach to promote the dispersion of CNCs through PLA matrix is the use of surface modification methods. The most widely explored surface modification techniques are acetylation (Cetin et al., 2009; Lin et al., 2011), esterification (Spinella et al., 2016; Yuan, Nishiyama, Wada, & Kuga, 2006), silylation (Andresen, Johansson, Tanem, & Stenius, 2006; Yu et al., 2015) and carboxymethylation (Aguir & M'Henni, 2006; Aulin, Johansson, Wågberg, & Lindström, 2010).

In addition to surface modification methods, several manufacturing processes have been investigated to promote the uniform dispersion of

* Corresponding author.
E-mail addresses: jamileh.shojaeiarani@ndsu.edu (J. Shojaeiarani), dilpreet.bajwa@ndsu.edu (D.S. Bajwa), nstark@fs.fed.us (N.M. Stark).

https://doi.org/10.1016/j.carbpol.2018.02.069
Received 10 November 2017; Received in revised form 9 February 2018; Accepted 22 February 2018
Available online 23 February 2018
0144-8617/

cellulose nanocrystals into hydrophobic polymers. Liquid feeding of cellulose-based nanoparticles into the PLA polymer during the extrusion process and the application of masterbatch films with high nanofiller concentration have been studied to improve the dispersion of nanoparticles in polymer matrix (Jonoobi, Harun, Mathew, & Oksman, 2010; Oksman, Mathew, Bondeson, & Kvien, 2006; Yang, Gardner, & Nader, 2013).

High concentrated masterbatch is mostly prepared through solvent casting technique. Solvent casting is a century-old methodology for nanocomposite films production. In this method, a polymer is first dissolved in a solvent and then fibers or filler are added to the solution. The solvent is then evaporated leaving behind thin nanocomposite film. Thin films with uniform thickness, maximum optical clarity, and low haze are some advantages of solvent casting technology (Anbukarasu, Sauvageau, & Elias, 2015; Hsu & Yao, 2014; Siemann, 2005).

Spin-coating method is extensively employed for fabrication of smooth polymeric coatings on flat substrates. In this method, the polymer solution is applied on a substrate which can be either static or rotating at a low speed (Hall, Underhill, & Torkelson, 1998; Mellbring, Kihlman Øiseth, Krozer, Lausmaa, & Hjertberg, 2001; Norrman, Ghanbari-Siahkali, & Larsen, 2005). Spin-coating has also been used to prepare open films of cellulose nanoparticles on different substrates to examine the influence of the substrate on the nanoparticles submonolayer (Herrera, Mathew, & Oksman, 2014; Kontturi, Thüne, Alexeev, & Niemantsverdriet, 2005). In the spin-coating method, thin films with the thickness of the order of micrometers are spread evenly over the substrate surface owing to centrifugal force and the surface tension of the solution. In this method, solvent evaporates simultaneously as the solution is applied on the substrate (Hall et al., 1998).

In spite of the broad use of the spin-coating method in thin film preparation, to the best of our knowledge, no one has used this technique for preparing masterbatches. Spin-coating method was introduced for the first time in this paper as masterbatch preparation technique and solvent casting method was considered as the reference method. Modified CNCs were prepared through physical attachment method introducing poly (ethylene oxide) to attach on the surface of CNCs. Composites were prepared using high shear melt compounding technique through extrusion followed by injection molding process. The agglomeration of cellulose nanocrystals in masterbatches and the corresponding composites were studied using scanning electron microscopy. In addition, crystallinity, thermal properties, and mechanical behavior of resultant composites were studied experimentally.

2. Experimental

2.1. Materials

Poly (lactic acid) (PLA 2002D, M_n = 98,000 g mol^{-1}) was supplied by NatureWorks LLC (Minnetonka, MN, USA). Polyethylene oxide (PEO, $M_n = 10^6$ g mol^{-1}) was purchased from Sigma-Aldrich (St. Louis, MO, USA). Cellulose nanocrystals (CNCs, dimensions of 150 nm length and 7 nm width) were provided by USDA-Forest Service, Forest Products Laboratory (Madison, WI, USA).

2.2. Cellulose nanocrystals modification

Physical attachment method was used to improve the interfacial bonding between CNCs and PLA. Poly (ethylene oxide) was introduced as a third polymer component attached to the surface of CNCs. It has been shown that there is an acceptable compatibility between PLA and PEO and the latter can improve the bio-degradation of PLA (NatureWorks, 2007). Modified CNCs (p-CNCs) were made from an aqueous mixture of 4% CNCs and 1% PEO suspension with the weight ratio of 4:1 (CNCs:PEO). The mixture was then freeze-dried for further use (Ben Azouz, Ramires, Van den Fonteyne, El Kissi, & Dufresne, 2011; Huang, Chen, & Chang, 2015).

2.3. Preparation of masterbatch

Chloroform was used as solvent in both methods to dissolve PLA and disperse p-CNCs. Masterbatch thin films with 15 wt% p-CNCs and 85 wt % of PLA were prepared through solvent casting and spin-coating techniques.

In both methods, PLA was dissolved in chloroform (30 wt%) under vigorous stirring at room temperature (24 °C) until the PLA pellets were fully dissolved. The p-CNCs were dispersed in chloroform (7.5 wt%) using homogenizer (IKA T50 ULTRA-TURRAX, Wilmington, NC, USA) for 5 min and then transferred to an ultrasonic probe (Misonix sonicator 3000; 550 W, 20 kHz, Vernon Hills, IL, USA) for 5 min to achieve a stable suspension. The dissolved PLA and dispersed p-CNCs solutions were then mixed together and stirred for 5 h at room temperature. In solvent casting method, the mixture was directly poured into Petri dishes and chloroform was allowed to evaporate at ambient temperature for 30 h.

In the second method, a spin-coater machine (WS-400-6NPP-LITE, North Wales, PA, USA) equipped with a vacuum chamber was used. The mixture was loaded in a syringe and injected through a needle (diameter = 500 μm) onto the center of the rotating glass substrate with 100 mm diameter, and spread evenly by the combination of centrifugal force and surface tension. To achieve the desired and even thickness of the films, the spinning speed was kept constant at 400 rpm for 180 s. The spin-coated films were dried out simultaneously as the solution was injected onto the substrate. The ultimate thickness of both masterbatch films was approximately 1.12 mm.

2.4. Preparation of PLA composite

Dried masterbatch films were chopped using a paper cutter (ACCO, Columbus, WI, USA) with the approximate size of 4 mm by 4 mm, premixed with PLA pellets and then diluted to final CNC concentrations of 1, 3, and 5 wt% using a twin-screw extruder (Krauss-Maffei Co., Florence, KY, USA). The barrel temperature for eight zones was set at 157, 157, 165, 162, 162, 162, 160, 160 °C (feed throat to die end), respectively, and the screw speed was set at 170 rpm. The extruded pellets were dried in an oven (Binder ED, Binder Inc., Bohemia, NY, USA) set at 80 °C for 24 h prior to processing in an injection molding machine. Injection molding machine (Technoplas Inc. model SIM-5080) was used to prepare composite samples. Samples were molded for tensile and impact tests according to ASTM D790 and ASTM D638 standards, respectively (ASTM D790-03, 2003; ASTM D638-03, 2008). All samples including pure PLA and composites went through the same extrusion and molding cycles. The samples obtained from injection molding machine with different material designations and compositions of PLA and p-CNCs are summarized in Table 1.

2.5. Morphological studies and surface behavior

2.5.1. Scanning electron microscopy (SEM) of masterbatch

The dispersion of p-CNCs in each masterbatch films was evaluated using scanning electron microscope (JSM-7600F, USA Inc., Peabody, MA, USA) operating at 15 kV. The SEM images were taken at a

Table 1
Codes and compositions details of composite samples.

Sample code	PLA (wt%)	CNCs (wt%)	PEO (wt%)	Method
PLA	100	0	0	Virgin
PLA-1CNC-so	99	0.94	0.06	Solvent casting
PLA-3CNC-so	97	2.8	0.2	Solvent casting
PLA-5CNC-so	95	4.7	0.3	Solvent casting
PLA-1CNC-sp	99	0.94	0.06	Spin-coating
PLA-3CNC-sp	97	2.8	0.2	Spin-coating
PLA-5CNC-sp	95	4.7	0.3	Spin-coating

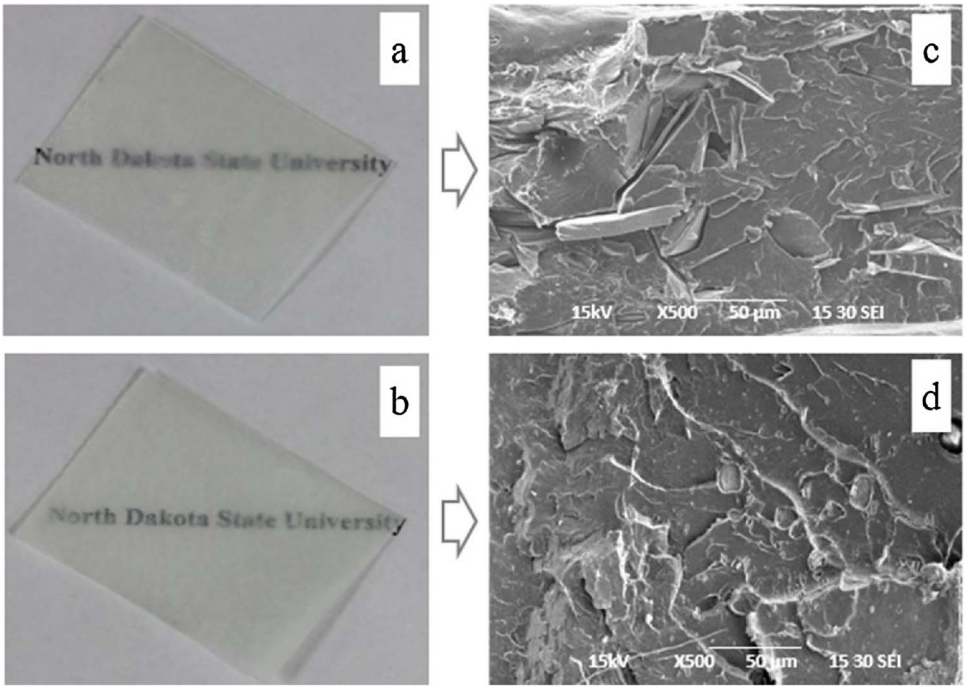

Fig. 1. Masterbatch films prepared from different methods: (a) solvent casting, (b) spin-coating, and SEM images of masterbatch films: (c) Solvent cast, (d) Spin-coated.

magnification of 500 from the cross section of masterbatches.

2.5.2. Scanning electron microscopy (SEM) of composites

The morphology of the impact-fractured surface of composites was examined using a scanning electron microscope (JSM-6010LA, USA Inc., Peabody, MA, USA) with an accelerating voltage of 10.0 kV at a magnification of 100. All samples were attached to the aluminum mounts using carbon adhesive tabs and coated with a conductive layer of carbon in a high-vacuum evaporative coater (Cressington, Ted Pella Inc., Redding, CA, USA).

2.6. Optical light microscopy

The dispersion quality and degree of self-aggregation of p-CNCs at composite samples was investigated using an optical microscope (Axiovert 40MAT, Carl Zeiss, Dublin, CA, USA). The average size of p-CNCs aggregates through PLA matrix was studied through iSolution DT software. For preparing thin films for the optical microscope, the composite extruded pellets were melted on a glass slide at 150 °C for 10 min and another glass slide was put on the melted samples as a cover glass to prepare a flat thin film for each formulation.

2.7. Differential scanning calorimeter (DSC)

DSC measurements were performed on DSC Q200 (TA Instruments, New Castle, DE, USA) over a temperature range from 25 to 200 °C at a heating rate of 1 °C/min and then held for 5 min, and then samples were cooled down to 25 °C at a cooling rate of 5 °C/min. The second heating was performed at the same range and heating rate to determine glass transition temperature (T_g), crystallization temperature (T_c), melting temperature (T_m). The Degree of crystallinity of samples were calculated using Eq. (1).

$$X_c = \left[\frac{\Delta H_m - \Delta H_c}{\Delta H_m^c}\right] \times \frac{100}{W_{PLA}} \quad (1)$$

here ΔH_m, ΔH_c, and ΔH_m^c are the melting enthalpy, cold crystallization enthalpy, and melting heat for pure crystalline PLA (93.6 J g^{-1}) respectively. WPLA is the weight fraction of PLA in the composite sample (Quero, Müller, Signori, Coltelli, & Bronco, 2012).

2.8. Dynamic mechanical analysis (DMA)

Thermomechanical behavior of PLA and composite samples were studied using a DMA Q800 (TA Instruments, New Castle, DE, USA) following ASTM D4065 (ASTM D4065-01, 2012). Measurements were carried out from 25 to 90 °C at a heating rate of 1 °C/min, with a fixed frequency of 1 Hz in a dual cantilever mode.

2.9. Mechanical properties of materials

Mechanical properties of composites including ultimate tensile strength, elongation at break, and modulus of elasticity were obtained from tensile test. The tensile testing was performed following ASTM D638 standard using an Instron universal testing machine (Model 5567, Norwood, MA, USA) (ASTM D638-03, 2008). Since the concentration and dispersion quality of CNCs in the PLA matrix can influence the toughness of the composites, the toughness of samples was calculated following ASTM D256 standard (ASTM D256-10, 2005). The tests were conducted on unnotched impact specimens using an Izod impact tester (Tinius Olsen, Model Impact 104, PA, USA).

2.10. Statistical analysis

The mean values and standard deviations of the mechanical properties of the samples were statistically analyzed by ANOVA and Tukey's test ($\alpha = 0.05$). The data was analyzed using Minitab software version 17 (Minitab Inc., State College, PA, USA). Eight replicates were used for each test.

3. Results and discussion

3.1. Morphological studies and surface behavior

3.1.1. Scanning electron microscopy (SEM) of masterbatch

The prepared masterbatches through solvent casting and spin-coating techniques and their corresponding cross sectional SEM

micrographs are shown in Fig. 1. The SEM images show that spin-coated masterbatch films exhibited smaller and well-dispersed p-CNCs aggregates in comparison with solvent cast masterbatches in which micrometric CNC aggregates can be observed. This behavior can be attributed to the application of centrifugal force through rotating substrate and surface tension against the attractive forces between p-CNCs in spin-coating process which inhibited the formation of p-CNCs aggregates.

The high evaporation rate and low essential time for vaporizing the solvent from thin films in spin-coating method, limited the movement of p-CNCs through PLA matrix and inhibited their assembly into micro-sized aggregates. Slower evaporation rate in solvent casting technique allows solvent molecules to exclude the nanoparticles and pushing them into closer proximity and leading to the formation of strong agglomerates. It was also observed that high evaporation rate in spin-coated masterbatches accelerated the drying process and consequently resulting in the formation of the air bubble on the surface of the masterbatch films.

3.1.2. Scanning electron microscopy (SEM) of composites

The impact-fractured surfaces of PLA composites were evaluated using SEM images (Fig. 2). Some small spherical particles can be observed on the fractured surfaces of solvent cast composites and PLA-5CNC-sp, indicating poor dispersion of p-CNCs through PLA matrix and low interaction between p-CNCs and PLA. However, a good dispersion was achieved in spin-coated composites with low p-CNC contents (1 and 3 wt%). Particularly, no aggregation was detected on the fracture surface of PLA-1CNC-sp (Fig. 2d). Given that the higher concentration of CNCs can result in greater aggregates (Shi et al., 2012; Spinella et al., 2015), we hypothesize that non-uniform dispersion of p-CNCs at the higher concentration can be attributed to inadequate shear or lower residence time in the twin screw extruder. Another factor that contributed to uneven dispersion is evaporation of the residual solvent and high viscosity of p-CNCs as reported in a recent study. It is reported that dispersion of CNCs in liquid feeding is influenced by percentage liquid phase, and liquid feeding rate (Herrera, Mathew, & Oksman, 2015; Strong, 2006). In this work, the presence of high amount of residual solvent associated with a large volume of spin-coated masterbatche pellets inhibited the uniform dispersion of 5% p-CNC in PLA matrix during the extrusion process.

The fractured surface corresponding to PLA-1CNC-sp and PLA-3CNC-sp was rougher and more irregular as compared to solvent cast composites with the same p-CNCs content. In general, the mechanical properties of samples can be correlated with the morphology of the composites and the rough and irregular impact-fractured surface can be an indication of tough materials. The presence of plenty of fracture lines on the impact fractured surface of PLA-1CNC-sp and PLA-3CNC-sp, can be considered as an indication of high toughness in materials (Gao & Qiang, 2017; Todo & Takayama, 2011). To have more information on samples toughness, impact strength was also studied.

3.2. Optical light microscopy

Optical microscopy images are illustrated in Fig. 3. The average size of p-CNCs aggregates increased with increasing the p-CNC loading in composites. The number of relatively big aggregates ($> 2.5\,\mu m$) increased with increasing p-CNC content in composite samples prepared via solvent casting and spin-coating routes.

With respect to the agglomeration size, spin-coated composites with 1 and 3% p-CNCs contents exhibited smaller p-CNCs aggregates in comparison with composites prepared using solvent cast masterbatch. This observation can be attributed to well-embedded p-CNCs in masterbatch films which lowered the possibility of forming p-CNCs aggregates in composites during extrusion process (Fig. 1). However, dispersion was slightly better in solvent cast composites with 5% p-CNCs loading.

3.3. Differential scanning calorimeter (DSC)

Fig. 4 illustrates the DSC heating scan thermograms of PLA and composite samples observed from second heating scans. The DSC thermograms show that there is a variation in the exothermic peak value and position related to cold crystallization for different samples confirming that different samples acquire different mobility to rearrange their crystal structure. All samples possessed single crystallization temperature (T_c), proving the presence of single homogeneous phase through the heating process. Interestingly, all samples except PLA-3CNC-sp and PLA-5CNC-sp possessed melting endotherms with two distinct peaks which can be attributed either to different crystal structures in the composite sample or the melt-recrystallization mechanism (Martin & Averous, 2001; Nijenhuis, Colstee, Grijpma, & Pennings, 1996; Yasuniwa, Sakamo, Ono, & Kawahara, 2008). The corresponding DSC thermal parameters are listed in Table 2. It can be observed that the glass transition temperature (T_g) was shifted to higher

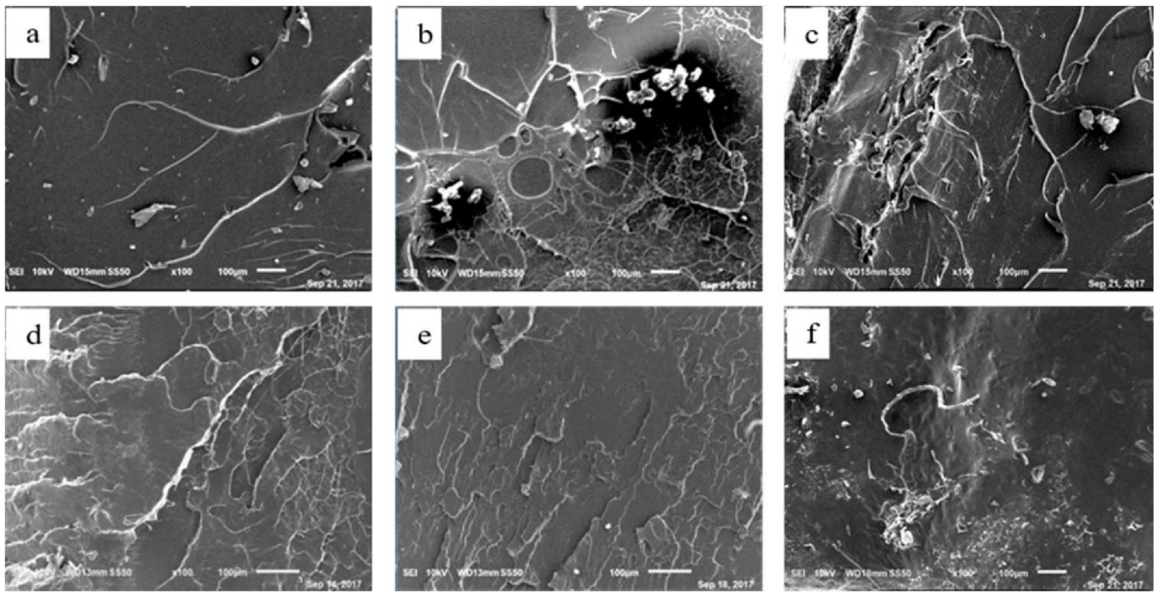

Fig. 2. SEM micrographs of PLA-CNC composites: a) PLA-1CNC-so, b) PLA-3CNC-so, c) PLA-5CNC-so, d) PLA-1CNC-sp, e) PLA-3CNC-sp and f) PLA-5CNC-sp.

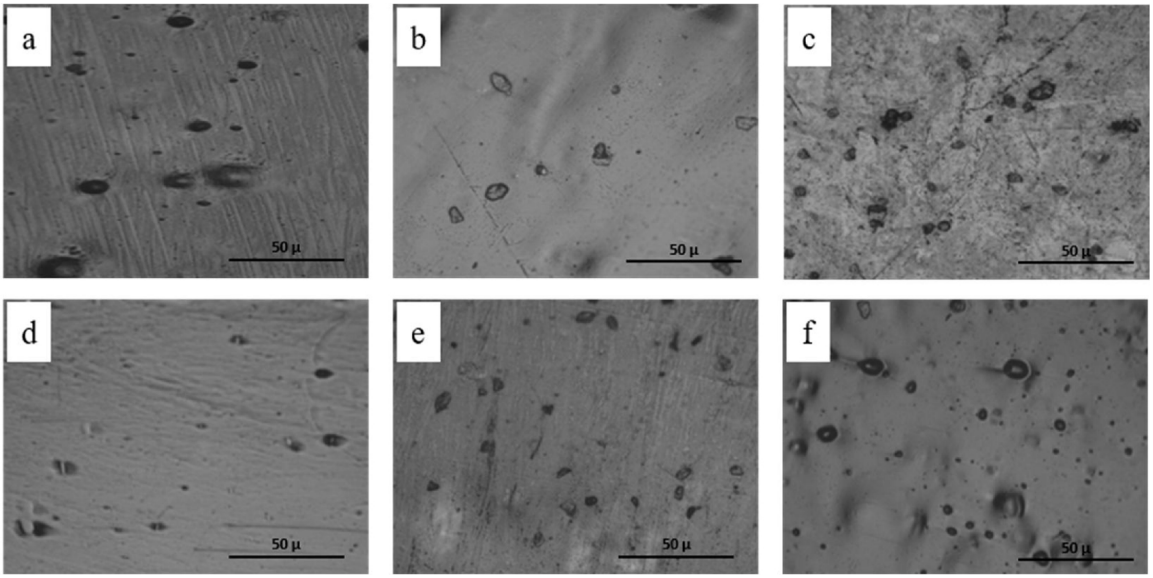

Fig. 3. Optical micrographs of PLA-CNC composites: a) PLA-1CNC-so, b) PLA-3CNC-so, c) PLA-5CNC-so, d) PLA-1CNC-sp, e) PLA-3CNC-sp and f) PLA-5CNC-sp.

values in all composites compared to pure PLA and the average T_g in solvent cast and spin-coated composites increased by 6% and 4%, respectively. The observed differences in the thermal characteristics between composite samples and pure PLA can be attributed to the influence of incorporating p-CNC and chloroform on the actual composition and characteristics of the final products.

The average crystallization peak temperature decreased by 13% and 18% for solvent cast and spin coated composites, respectively. The observed decreases in T_c could be attributed to the influence of PEO incorporation and the presence of residual solvent in the specimens. Amount of residual solvent in each masterbatch right before the extrusion process were measured and the results showed the presence of 8.65% residual solvent in spin coated masterbatches compared to 1.37% in solvent cast masterbatches.

Higher decline in T_C was observed in spin-coated composites as compared to solvent cast samples. This behavior can be attributed to the application of well dispersed p-CNCs through PLA matrix as heterogeneous nucleus in lowering the cold crystallization temperature and facilitating the formation of organized structure (Du, Wu, Yan, Kortschot, & Farnood, 2014; Halász & Csóka, 2013). In addition, considering the drying process, spin-coated masterbatches dried in less time compared to solvent cast masterbatches, therefore, more decrease in T_c was observed in spin-coated composites.

Table 2
Thermal properties of PLA and composite samples.

Sample code	T_g (°C)	T_c (°C)	T_m (°C)	X%
PLA	50.16	103.98	155.06	3.99
PLA-1CNC-so	53.66	91.15	154.88	9.82
PLA-3CNC-so	52.77	91.08	152.84	12.49
PLA-5CNC-so	53.24	90.05	152.68	7.21
PLA-1CNC-sp	50.70	84.29	150.28	11.34
PLA-3CNC-sp	52.33	85.41	155.02	26.38
PLA-5CNC-sp	53.65	84.92	154.52	19.97

For all composite samples, the degree of crystallinity increased significantly with an increase in the p-CNCs content. In solvent cast and spin-coated composites the average degree of crystallinity increased by 147% and 380% in comparison with pure PLA, respectively.

The observed improvement in degree of crystallinity in composites was due to the presence of the p-CNCs and their nucleation effect (Fortunati, Armentano, Zhou, Iannoni et al., 2012). In each set of samples, the highest degree of crystallinity was observed in composites with 3 wt% p-CNCs and decreased with increasing p-CNCs content, suggesting the formation of p-CNCs aggregates at PLA-5CNCs.

The observation of higher crystallinity in spin-coated composites as

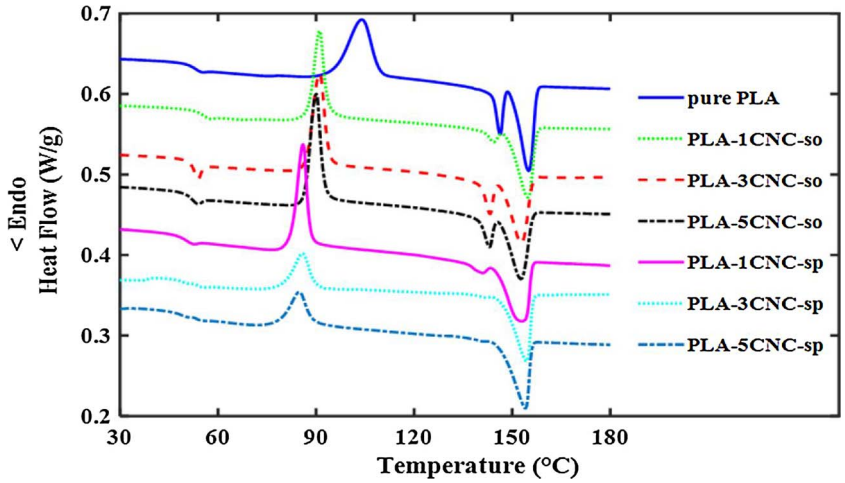

Fig. 4. DSC curves during the second heating scan of PLA and composites.

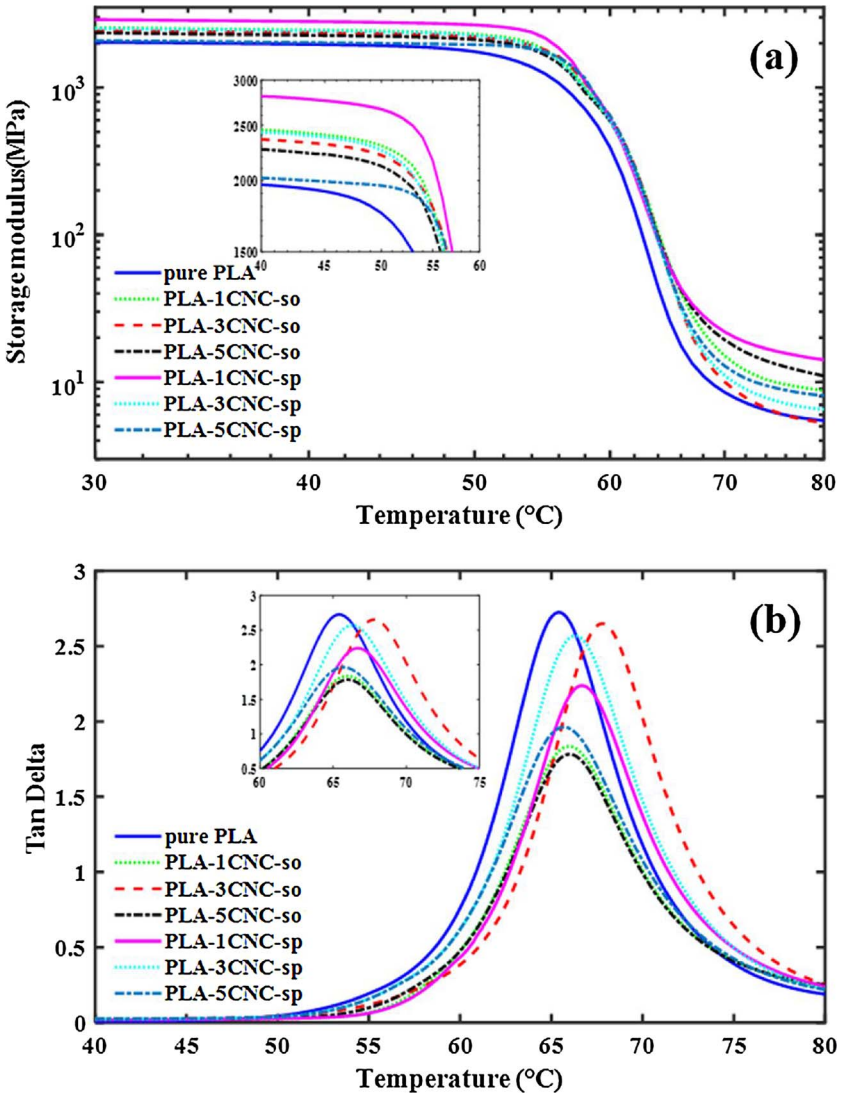

Fig. 5. Storage modulus (a) and Tan δ (b) as a function of temperature of PLA and composites.

compared to solvent cast samples were in agreement with another research that reported partial crystallization of amorphous molecules in the solvent cast films (Hsu & Yao, 2014). More uniform dispersion of p-CNCs in spin-coat composites led to the formation of higher attraction of p-CNCs in PLA matrix and induced a higher nucleation agent effect (Arrieta et al., 2014; Gupta et al., 2017; Tyona, 2013). As the optical micrographs suggested, the smaller CNCs aggregates in spin-coated composites resulted in a high number of nucleating sites and improving the degree of crystallinity. At solvent cast composites, lower degree of crystallinity was due to p-CNCs' agglomeration in PLA matrix (Fig. 3).

3.4. Dynamic mechanical analysis (DMA)

The stiffness of composites at elevated temperatures was evaluated through DMA test. Fig. 5 illustrates the storage modulus and tan δ as a function of temperature for pure PLA and composites. All samples exhibited a typical behavior of a semi-crystalline polymer with a large drop in storage modulus corresponding to their glass transition region (T_g). It can be observed that the addition of p-CNCs led to an improvement in the storage modulus of composites as compared to pure PLA in the glassy state. In lower p-CNCs contents (1 and 3 wt%), spin-coated composites exhibited higher storage modulus in comparison with solvent cast composites. In particular, storage modulus was increased by 29%, 21%, and 31% with increasing the p-CNCs content in solvent cast samples, and in the case of spin-coated composites it was improved by 49%, 24%, and 4% as compared to pure PLA. These results were in a good agreement with the microscope observations, and confirming the better p-CNCs dispersion in spin-coated composites at lower p-CNCs contents (Fig. 3).

From DMA results, tan δ peak temperature indicates the glass transition temperatures (T_g) of materials. It can be observed that the addition of p-CNCs slightly shifted the tan δ peaks toward higher temperature, however, the addition of p-CNCs did not have a significant effect on T_g and all samples exhibited T_g in the regions between 64 and 67 °C. In particular, the average T_g increased by 5% and 3% for solvent cast and spin-coated composites. The results on T_g showed that T_g from DSC and DMA observations methods had the same trend.

The viscoelastic behavior of samples was examined through the peak values of the tan δ curves in Fig. 5b. The peak values of the tan δ exhibits the viscoelastic behavior of materials and the dissipated energy by sample through deformation (Chartoff, Menczel, & Dillman, 2009). In composites the lower tan δ peak values indicates the enhancement in interfacial bonding between fibers and matrix (Pothan, Oommen, & Thomas, 2003). All composites exhibited lower peak value for tan δ as compared to pure PLA. The average peak value for tan δ decreased by 18% and 22% for solvent cast and spin-coated composites, respectively. This result can be attributed to the restrictive effect of p-CNCs through PLA matrix to the segmental motions of the polymer molecules during

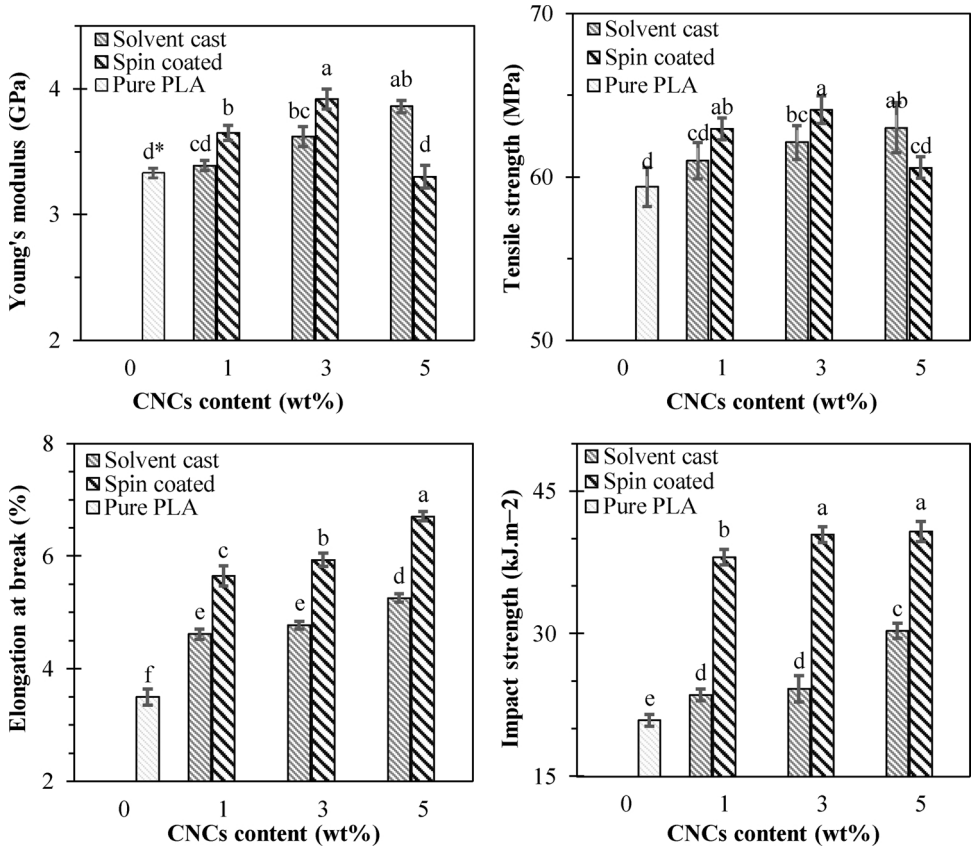

Fig. 6. Mechanical properties of PLA and composite samples (*bars in each graph sharing same superscript letter are not significantly different at 5% significance level).

the transition and resulting in more elastic response of materials (Hassan, Wei, Jiao, & Muhuo, 2013).

3.5. Mechanical characteristics

It was shown that the mechanical properties in composites are governed by nanofiller dispersion through the matrix, interfacial properties, and polymer crystallinity (Grady, 2010; Paul & Robeson, 2008). The mechanical behavior of samples with different formulations was evaluated by tensile and impact tests. The mean and standard deviations of the mechanical properties of PLA and composites are shown in Fig. 6. In general, the incorporation of p-CNCs increased Young's modulus, tensile strength, elongation at break, and impact strength, although, no significant improvement was observed in the case of Young's modulus and tensile strength for solvent cast composites. Significantly higher Young's modulus and ultimate tensile strength in PLA-1CNC-sp and PLA-3CNC-sp demonstrated that more uniform p-CNCs dispersion in spin-coated composites with lower p-CNCs loadings (i.e. 1 wt% and 3 wt%) has formed a stronger interfacial adhesion between PLA and p-CNCs and resulted in an improvement in mechanical properties of spin-coated composites (Fig. 3). Similar findings were reported where more uniform CNCs dispersion resulted in higher tensile stress and Young's modulus in PLA- based nanocomposites (Fortunati, Armentano, Zhou, Puglia et al., 2012; Pracella, Haque, & Puglia, 2014)

As already observed on DSC analysis, the incorporation of p-CNCs improved the polymer crystallization in composites and resulted in an enhancement of Young's modulus and tensile strength because the composites' rigidity also improved. In general, the higher the degree of crystallinity, the harder the composite. These results are consistent with previous published works on electrospun bio-nanocomposite mats from PLA and CNCs (Shi et al., 2012) and PLA-lignin coated CNCs nanocomposites (Gupta et al., 2017) which indicated the same correlation between composite crystallinity and strength.

There was a significant improvement in the elongation at break and impact strength for all composites prepared via spin-coating and solvent casting routes as compared to pure PLA. It is difficult to describe why incorporation of p-CNCs in PLA had so large influence on elongation at break and impact strength since different factors such as structure and incorporation of PEO could affect the mechanical properties of samples. However, similar results have reported by adding cellulose nanowiskers to PLA (Oksman et al., 2006). In particular, spin-coated composites possessed higher elongation at break and impact strength than solvent cast composites at all p-CNCs loadings. These results confirmed the previous conclusion drawn from rough and irregular fractured surface in spin-coat composites observed in SEM images (Fig. 2).

4. Conclusion

We have described a versatile spin-coating technology for masterbatch preparation. Modified cellulose nanocrystals were successfully incorporated in PLA by preparing masterbatch through spin-coating and solvent casting methods. SEM micrographs of masterbatches revealed more homogenous and uniform p-CNCs dispersion in PLA-CNC-sp samples compared to PLA-CNC-so with low CNCs concentrations. The SEM investigations on fracture surface confirmed the difference in fracture surfaces in solvent cast and spin-coated composite. The difference can be attributed to the effect of masterbatch preparation methods on p-CNCs distribution and their interaction with PLA matrix. DSC results confirmed the increase of the crystallinity for nanocomposite samples compared to pure PLA; in which the spin-coated composites exhibited higher degree of crystallinity than solvent cast samples. This behavior can be attributed to partial crystallization of amorphous molecules in the solvent cast films. Spin-coated composites exhibited higher mechanical properties and storage modulus at lower p-CNCs contents (1 and 3%) and higher ductility for all samples. The

presence of air bubbles on the surface of spin-coated masrterbatches observed in optical microscopy images resulted from high evaporation rate of the solvent in spin-coating process. Lower thermal characteristics in spin-coated composites resulted from the residual solvent in composites was due to short time for drying process. In general, these results show huge potential for using different manufacturing methods along with chemical modification methods to overcome the major obstacles to producing PLA-CNCs composites on a commercial scale.

Acknowledgement

The authors are grateful for the support and funding from National Science Foundation, ND EPSCoR (grant No.11A1355466) for conducting this research.

References

Aguir, C., & M'Henni, M. F. (2006). Experimental study on carboxymethylation of cellulose extracted from Posidonia oceanica. *Journal of Applied Polymer Science, 99*(4), 1808–1816.

Anbukarasu, P., Sauvageau, D., & Elias, A. (2015). Tuning the properties of polyhydroxybutyrate films using acetic acid via solvent casting. *Scientific Reports, 5*, 17884.

Andresen, M., Johansson, L.-S., Tanem, B. S., & Stenius, P. (2006). Properties and characterization of hydrophobized microfibrillated cellulose. *Cellulose, 13*(6), 665–677.

Arrieta, M., Fortunati, E., Dominici, F., Rayón, E., López, J., & Kenny, J. (2014). Multifunctional PLA–PHB/cellulose nanocrystal films: Processing, structural and thermal properties. *Carbohydrate Polymers, 107*, 16–24.

ASTM D790-03 (2003). *Standard test methods for flexural properties of unreinforced and reinforced plastics and electrical insulating materials.* West Conshohocken, PA: ASTM International.

ASTM D256-10 (2005). *Standard test method for determining the Izod pendulum impact resistance of plastics.* West Conshohocken, PA: ASTM International.

ASTM D638-03 (2008). *Standard test method for tensile properties of plastics.* West Conshohocken, PA: ASTM International.

ASTM D4065-01 (2012). *Standard practice for plastics: Dynamic mechanical properties: Determination and report of procedures*West Conshohocken, PA: ASTM International.

Aulin, C., Johansson, E., Wågberg, L., & Lindström, T. (2010). Self-organized films from cellulose I nanofibrils using the layer-by-layer technique. *Biomacromolecules, 11*(4), 872–882.

Ben Azouz, K., Ramires, E. C., Van den Fonteyne, W., El Kissi, N., & Dufresne, A. (2011). Simple method for the melt extrusion of a cellulose nanocrystal reinforced hydrophobic polymer. *ACS Macro Letters, 1*(1), 236–240.

Brinchi, L., Cotana, F., Fortunati, E., & Kenny, J. (2013). Production of nanocrystalline cellulose from lignocellulosic biomass: Technology and applications. *Carbohydrate Polymers, 94*(1), 154–169.

Cetin, N. S., Tingaut, P., Özmen, N., Henry, N., Harper, D., Dadmun, M., & Sebe, G. (2009). Acetylation of cellulose nanowhiskers with vinyl acetate under moderate conditions. *Macromolecular Bioscience, 9*(10), 997–1003.

Chartoff, R. P., Menczel, J. D., & Dillman, S. H. (2009). *Dynamic mechanical analysis (DMA). Thermal analysis of polymers: Fundamentals and applications*387–495.

Cheng, Y., Deng, S., Chen, P., & Ruan, R. (2009). Polylactic acid (PLA) synthesis and modifications: A review. *Frontiers of Chemistry in China, 4*(3), 259–264.

De France, K. J., Chan, K. J., Cranston, E. D., & Hoare, T. (2016). Enhanced mechanical properties in cellulose nanocrystal–poly (oligoethylene glycol methacrylate) injectable nanocomposite hydrogels through control of physical and chemical cross-linking. *Biomacromolecules, 17*(2), 649–660.

Domenek, S., & Ducruet, V. (2016). *Characteristics and applications of PLA. Biodegradable and biobased polymers for environmental and biomedical applications*171–224.

Drumright, R. E., Gruber, P. R., & Henton, D. E. (2000). Polylactic acid technology. *Advanced Materials, 12*(23), 1841–1846.

Du, Y., Wu, T., Yan, N., Kortschot, M. T., & Farnood, R. (2014). Fabrication and characterization of fully biodegradable natural fiber-reinforced poly (lactic acid) composites. *Composites Part B: Engineering, 56*, 717–723.

Duran, N., Paula Lemes, A., & Seabra, A. B. (2012). Review of cellulose nanocrystals patents: Preparation, composites and general applications. *Recent Patents on Nanotechnology, 6*(1), 16–28.

Fortunati, E., Armentano, I., Zhou, Q., Iannoni, A., Saino, E., Visai, L., ... Kenny, J. (2012). Multifunctional bionanocomposite films of poly (lactic acid), cellulose nanocrystals and silver nanoparticles. *Carbohydrate Polymers, 87*(2), 1596–1605.

Fortunati, E., Armentano, I., Zhou, Q., Puglia, D., Terenzi, A., Berglund, L. A., & Kenny, J. (2012). Microstructure and nonisothermal cold crystallization of PLA composites based on silver nanoparticles and nanocrystalline cellulose. *Polymer Degradation and Stability, 97*(10), 2027–2036.

Gao, H., & Qiang, T. (2017). Fracture surface morphology and impact strength of cellulose/PLA composites. *Materials, 10*(6), 624.

Grady, B. P. (2010). Recent developments concerning the dispersion of carbon nanotubes in polymers. *Macromolecular Rapid Communications, 31*(3), 247–257.

Gupta, A., Simmons, W., Schueneman, G. T., Hylton, D., & Mintz, E. A. (2017). Rheological and thermo-mechanical properties of poly (lactic acid)/lignin-coated cellulose nanocrystal composites. *ACS Sustainable Chemistry & Engineering, 5*(2), 1711–1720.

Halász, K., & Csóka, L. (2013). Plasticized biodegradable poly (lactic acid) based composites containing cellulose in micro-and nanosize. *Journal of Engineering, 2013*.

Hall, D. B., Underhill, P., & Torkelson, J. M. (1998). Spin coating of thin and ultrathin polymer films. *Polymer Engineering & Science, 38*(12), 2039–2045.

Hamad, W. (2006). On the development and applications of cellulosic nanofibrillar and nanocrystalline materials. *The Canadian Journal of Chemical Engineering, 84*(5), 513–519.

Hassan, E., Wei, Y., Jiao, H., & Muhuo, Y. (2013). Dynamic mechanical properties and thermal stability of poly (lactic acid) and poly (butylene succinate) blends composites. *Journal of Fiber Bioengineering and Informatics, 6*(1), 85–94.

Herrera, M. A., Mathew, A. P., & Oksman, K. (2014). Gas permeability and selectivity of cellulose nanocrystals films (layers) deposited by spin coating. *Carbohydrate Polymers, 112*, 494–501.

Herrera, N., Mathew, A. P., & Oksman, K. (2015). Plasticized polylactic acid/cellulose nanocomposites prepared using melt-extrusion and liquid feeding: Mechanical, thermal and optical properties. *Composites Science and Technology, 106*, 149–155.

Hsu, S.-T., & Yao, Y. L. (2014). Effect of film formation method and annealing on morphology and crystal structure of poly (L-lactic acid) films. *Journal of Manufacturing Science and Engineering, 136*(2), 021006.

Huang, J., Chen, Y., & Chang, P. R. (2015). *Surface modification of cellulose nanocrystals for nanocomposites. Surface modification of biopolymers*258.

Jamshidian, M., Tehrany, E. A., Imran, M., Jacquot, M., & Desobry, S. (2010). Poly-lactic acid: Production, applications, nanocomposites, and release studies. *Comprehensive Reviews in Food Science and Food Safety, 9*(5), 552–571.

Jonoobi, M., Harun, J., Mathew, A. P., & Oksman, K. (2010). Mechanical properties of cellulose nanofiber (CNF) reinforced polylactic acid (PLA) prepared by twin screw extrusion. *Composites Science and Technology, 70*(12), 1742–1747.

Klemm, D., Kramer, F., Moritz, S., Lindström, T., Ankerfors, M., Gray, D., & Dorris, A. (2011). Nanocelluloses: A new family of nature-based materials. *Angewandte Chemie International Edition, 50*(24), 5438–5466.

Kontturi, E., Thüne, P., Alexeev, A., & Niemantsverdriet, J. (2005). Introducing open films of nanosized cellulose—Atomic force microscopy and quantification of morphology. *Polymer, 46*(10), 3307–3317.

López de Dicastillo, C., Garrido, L., Alvarado, N., Romero, J., Palma, J. L., & Galotto, M. J. (2017). Improvement of polylactide properties through cellulose nanocrystals embedded in poly (vinyl alcohol) electrospun nanofibers. *Nanomaterials, 7*(5), 106.

Li, X., Guo, C., Liu, X., Liu, L., Bai, J., Xue, F., ... Chu, C. (2014). Impact behaviors of polylactic acid based biocomposite reinforced with unidirectional high-strength magnesium alloy wires. *Progress in Natural Science: Materials International, 24*(5), 472–478.

Lim, L.-T., Auras, R., & Rubino, M. (2008). Processing technologies for poly (lactic acid). *Progress in Polymer Science, 33*(8), 820–852.

Lin, N., Huang, J., Chang, P. R., Feng, J., & Yu, J. (2011). Surface acetylation of cellulose nanocrystal and its reinforcing function in poly (lactic acid). *Carbohydrate Polymers, 83*(4), 1834–1842.

Ljungberg, N., & Wesslén, B. (2005). Preparation and properties of plasticized poly (lactic acid) films. *Biomacromolecules, 6*(3), 1789–1796.

Martínez-Sanz, M., Lopez-Rubio, A., & Lagaron, J. M. (2012). Optimization of the dispersion of unmodified bacterial cellulose nanowhiskers into polylactide via melt compounding to significantly enhance barrier and mechanical properties. *Biomacromolecules, 13*(11), 3887–3899.

Martin, O., & Averous, L. (2001). Poly (lactic acid): Plasticization and properties of biodegradable multiphase systems. *Polymer, 42*(14), 6209–6219.

Masutani, K., & Kimura, Y. (2014). *PLA synthesis. From the monomer to the polymer*.

Mellbring, O., Kihlman Øiseth, S., Krozer, A., Lausmaa, J., & Hjertberg, T. (2001). Spin coating and characterization of thin high-density polyethylene films. *Macromolecules, 34*(21), 7496–7503.

Nam, J. Y., Sinha Ray, S., & Okamoto, M. (2003). Crystallization behavior and morphology of biodegradable polylactide/layered silicate nanocomposite. *Macromolecules, 36*(19), 7126–7131.

NatureWorks, L (2007). *Technology focus report: Blends of PLA with other thermoplastics*USA: NatureWorks, L.

Nijenhuis, A., Colstee, E., Grijpma, D., & Pennings, A. (1996). High molecular weight poly (L-lactide) and poly (ethylene oxide) blends: Thermal characterization and physical properties. *Polymer, 37*(26), 5849–5857.

Norrman, K., Ghanbari-Siahkali, A., & Larsen, N. (2005). 6 Studies of spin-coated polymer films. *Annual Reports Section C(Physical Chemistry), 101*, 174–201.

Oksman, K., Skrifvars, M., & Selin, J.-F. (2003). Natural fibres as reinforcement in polylactic acid (PLA) composites. *Composites Science and Technology, 63*(9), 1317–1324.

Oksman, K., Mathew, A. P., Bondeson, D., & Kvien, I. (2006). Manufacturing process of cellulose whiskers/polylactic acid nanocomposites. *Composites Science and Technology, 66*(15), 2776–2784.

Paul, D., & Robeson, L. M. (2008). Polymer nanotechnology: Nanocomposites. *Polymer, 49*(15), 3187–3204.

Pothan, L. A., Oommen, Z., & Thomas, S. (2003). Dynamic mechanical analysis of banana fiber reinforced polyester composites. *Composites Science and Technology, 63*(2), 283–293.

Pracella, M., Haque, M. M.-U., & Puglia, D. (2014). Morphology and properties tuning of PLA/cellulose nanocrystals bio-nanocomposites by means of reactive functionalization and blending with PVAc. *Polymer, 55*(16), 3720–3728.

Quero, E., Müller, A. J., Signori, F., Coltelli, M. B., & Bronco, S. (2012). Isothermal cold-crystallization of PLA/PBAT blends with and without the addition of acetyl tributyl citrate. *Macromolecular Chemistry and Physics, 213*(1), 36–48.

Shi, X., Jiang, J., Sun, L., & Gan, Z. (2011). Hydrolysis and biomineralization of porous

PLA microspheres and their influence on cell growth. *Colloids and Surfaces B: Biointerfaces, 85*(1), 73–80.
Shi, Q., Zhou, C., Yue, Y., Guo, W., Wu, Y., & Wu, Q. (2012). Mechanical properties and in vitro degradation of electrospun bio-nanocomposite mats from PLA and cellulose nanocrystals. *Carbohydrate Polymers, 90*(1), 301–308.
Siemann, U. (2005). *Solvent cast technology–A versatile tool for thin film production. Scattering methods and the properties of polymer materials*307–316.
Spinella, S., Re, G. L., Liu, B., Dorgan, J., Habibi, Y., Leclere, P., ... Gross, R. A. (2015). Polylactide/cellulose nanocrystal nanocomposites: Efficient routes for nanofiber modification and effects of nanofiber chemistry on PLA reinforcement. *Polymer, 65*, 9–17.
Spinella, S., Maiorana, A., Qian, Q., Dawson, N. J., Hepworth, V., McCallum, S. A., ... Gross, R. A. (2016). Concurrent cellulose hydrolysis and esterification to prepare a surface-modified cellulose nanocrystal decorated with carboxylic acid moieties. *ACS Sustainable Chemistry & Engineering, 4*(3), 1538–1550.
Strong, A. B. (2006). *Plastics: Materials and processing* (3rd ed.). New Jersey, Columbus, Ohio: Prentice Hall.
Sullivan, E. M., Moon, R. J., & Kalaitzidou, K. (2015). Processing and characterization of cellulose nanocrystals/polylactic acid nanocomposite films. *Materials, 8*(12), 8106–8116.
Todo, M., & Takayama, T. (2011). *Fracture mechanisms of biodegradable PLA and PLA/PCL blends. Biomaterials-physics and chemistry*. InTech.
Tyona, M. (2013). A theoritical study on spin coating technique. *Advances in Materials Research, 2*(4), 195–208.
Yang, H. S., Gardner, D. J., & Nader, J. W. (2013). Morphological properties of impact fracture surfaces and essential work of fracture analysis of cellulose nanofibril-filled polypropylene composites. *Journal of Applied Polymer Science, 128*(5), 3064–3076.
Yasuniwa, M., Sakamo, K., Ono, Y., & Kawahara, W. (2008). Melting behavior of poly (l-lactic acid): X-ray and DSC analyses of the melting process. *Polymer, 49*(7), 1943–1951.
Yoon, C. S., & Ji, D. S. (2003). The effects of blend composition and blending time on the ester interchange reaction and tensile properties of PLA/LPCL/HPCL blends. *Fibers and Polymers, 4*(2), 59–65.
Yu, H.-Y., Qin, Z.-Y., Liu, Y.-N., Chen, L., Liu, N., & Zhou, Z. (2012). Simultaneous improvement of mechanical properties and thermal stability of bacterial polyester by cellulose nanocrystals. *Carbohydrate Polymers, 89*(3), 971–978.
Yu, H.-Y., Chen, R., Chen, G.-Y., Liu, L., Yang, X.-G., & Yao, J.-M. (2015). Silylation of cellulose nanocrystals and their reinforcement of commercial silicone rubber. *Journal of Nanoparticle Research, 17*(9), 361.
Yuan, H., Nishiyama, Y., Wada, M., & Kuga, S. (2006). Surface acylation of cellulose whiskers by drying aqueous emulsion. *Biomacromolecules, 7*(3), 696–700.